1-1-2011

Potential Fossil Endoliths in Vesicular Pillow Basalt, Coral Patch Seamount, Eastern North Atlantic Ocean

Barbara Cavalazzi
University of Johannesburg

Frances Westall
Centre de biophysique moléculaire

Sherry L. Cady
Portland State University

Roberto Barbieri
Università di Bologna

Frédéric Foucher
Centre de biophysique moléculaire

Citation Details

Cavalazzi, B., Westall, F., Cady, S. L., Barbieri, R., & Foucher, F. (2011). Potential Fossil Endoliths in Vesicular Pillow Basalt, Coral Patch Seamount, Eastern North Atlantic Ocean. [Article]. Astrobiology, 11(7), 619-632.

ASTROBIOLOGY
Volume 11, Number 7, 2011

DOI: 10.1089/ast.2011.0657

Potential Fossil Endoliths in Vesicular Pillow Basalt, Coral Patch Seamount, Eastern North Atlantic Ocean

Barbara Cavalazzi,[1,2] Frances Westall,[2] Sherry L. Cady,[3] Roberto Barbieri,[4] and Frédéric Foucher[2]

Abstract

The chilled rinds of pillow basalt from the Ampère–Coral Patch Seamounts in the eastern North Atlantic were studied as a potential habitat of microbial life. A variety of putative biogenic structures, which include filamentous and spherical microfossil-like structures, were detected in K-phillipsite–filled amygdules within the chilled rinds. The filamentous structures ($\sim$2.5 μm in diameter) occur as K-phillipsite tubules surrounded by an Fe-oxyhydroxide (lepidocrocite) rich membranous structure, whereas the spherical structures (from 4 to 2 μm in diameter) are associated with Ti oxide (anatase) and carbonaceous matter.

Several lines of evidence indicate that the microfossil-like structures in the pillow basalt are the fossilized remains of microorganisms. Possible biosignatures include the carbonaceous nature of the spherical structures, their size distributions and morphology, the presence and distribution of native fluorescence, mineralogical and chemical composition, and environmental context. When taken together, the suite of possible biosignatures supports the hypothesis that the fossil-like structures are of biological origin. The vesicular microhabitat of the rock matrix is likely to have hosted a cryptoendolithic microbial community. This study documents a variety of evidence for past microbial life in a hitherto poorly investigated and underestimated microenvironment, as represented by the amygdules in the chilled pillow basalt rinds. This kind of endolithic volcanic habitat would have been common on the early rocky planets in our Solar System, such as Earth and Mars. This study provides a framework for evaluating traces of past life in vesicular pillow basalts, regardless of whether they occur on early Earth or Mars. Key Words: Fossil microbes—Microhabitat—Vesicular pillow basalt. Astrobiology 11, 619–632.

1. Introduction

The oceanic lithosphere contributes significantly to biogeochemical cycling and the amount of biomass and biodiversity on Earth. It is also an important habitat for microbial life (Furnes and Staudigel, 1999; Furnes *et al.*, 2007; Santelli *et al.*, 2008; Staudigel *et al.*, 2008; McLoughlin *et al.*, 2009; Nielsen and Fisk, 2010). When the temperature of newly formed oceanic rocks drops to values that become tolerable for life, which is estimated to be less than 121–122°C (Takai *et al.*, 2001; Kashefi and Lovley, 2003), they can be colonized by microbial communities that utilize the inorganic elements and compounds of the rocky substratum as energy sources (Thorseth *et al.*, 1995). A wide variety of evidence, which includes the presence of fossilized microbes, spherical and tubular alteration cavities, and geochemical and molecular signatures consistent with microbial remains and metabolisms, is commonly associated with bioalteration of modern and ancient oceanic volcanic glass (for a comprehensive review see Staudigel *et al.*, 2008). Chemolithoautotrophic microorganisms have an affinity for many of the bioessential elements (*e.g.*, Fe^{2+}, Mn^{4+}, SO_4^{2-}, CO_2) present in basaltic silicates, which include olivine, pyroxene, feldspar, and hornblende (Fisk *et al.*, 2006, and references therein). Alteration of the silicate minerals as a result of weathering and microbial extraction releases the metabolically significant cations (Kostka *et al.*, 2002; Kim *et al.*, 2004). Bioalteration of the glassy basalts, which develops progressively along fracture surfaces and in and around vesicles produced by degassing, is accompanied by the formation of authigenic phases (*e.g.*, smectite and phillipsite) in the zone of alteration. Staudigel and coworkers (2008) presented a schematic model that illustrates the developmental stages and variety of mechanisms involved in microbial alteration of volcanic glasses.

[1]Department of Geology, University of Johannesburg, Johannesburg, South Africa.
[2]Centre de Biophysique Moléculaire–CNRS, Orléans, France.
[3]Department of Geology, Portland State University, Portland, Oregon, USA.
[4]Dipartimento di Scienze della Terra e Geologico-Ambientali, Università di Bologna, Bologna, Italy.

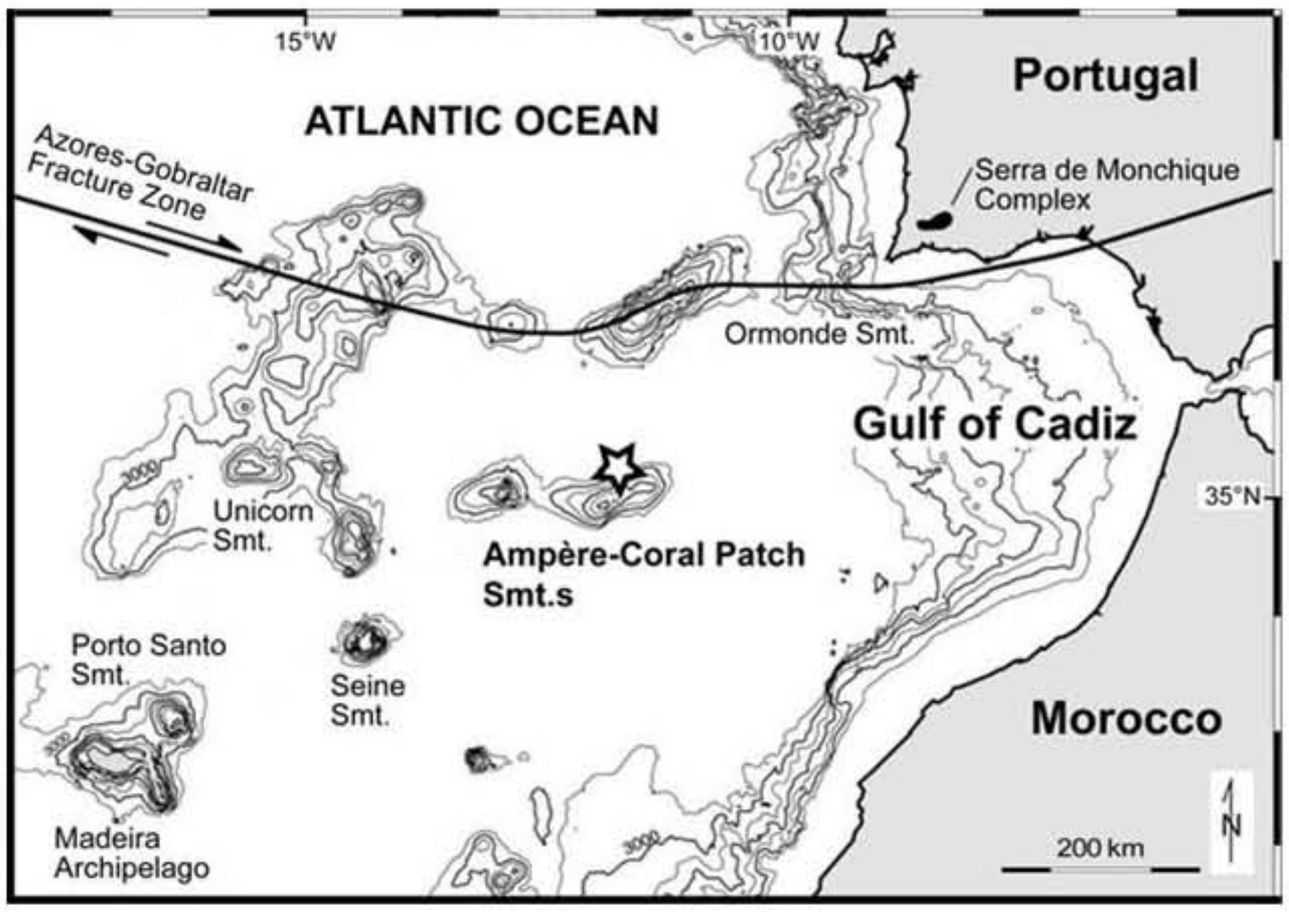

FIG. 1. Location map of sample site (star). The sample studied was dredged from the flank of Coral Patch Seamount (34°58.310 N to 34°56.773, 11°57.323 W to 11°57.140; water depth 1018 m) during the SWIM2004 scientific cruise in Gulf of Cadiz, Atlantic Ocean. The bathymetric map of seamounts and islands in the eastern North Atlantic Ocean is modified from Geldmacher and Hoernle (2000).

The primary glassy rinds of basalts provide a microbial habitat for endoliths, organisms that reside in the interior of rocks, and euendoliths, microbes that actively bore into the rock substratums and create microtubular cavities (McLoughlin *et al.*, 2007). Chemical alteration of the glassy rinds of seafloor basalts and of extrusive volcanic rock increases the range of microenvironments that could support such microbial communities. The diversity of glassy habitats supports communities of epiliths (eukaryotic and prokaryotic microorganisms that live by attaching themselves to the external surfaces of rocks), chasmoendoliths (endoliths that inhabit fissures and cracks in rocks), and cryptoendoliths (endoliths that are hypothesized to favor the colonization of rocks that have preexisting interstices and porous structures, *sensu* Santelli *et al.*, 2008).

Recent studies have shown that prokaryotes and eukaryotes also inhabit the primary and alteration rinds of crystalline volcanic rocks. Schumann *et al.* (2004) described putative fossilized fungal life in vesicles of deep oceanic basalt crust collected from a site in the North Pacific (ODP Site 1224). Connell *et al.* (2009) described fungi they discovered on the surfaces of basalts that formed relatively recently at a still-active deep-sea volcano (Vailulu'u Seamount, Samoa). Ivarsson *et al.* (2008) reported the discovery of fossil chasmoendoliths in zeolite-filled veins associated with subseafloor basaltic rocks sampled at the Emperor Seamounts in the Pacific Ocean. Peckmann *et al.* (2008) and Eickmann *et al.* (2009) found fossil evidence of marine cryptoendolithic prokaryotes within the carbonate amygdules (mineral-filled vesicles) of Devonian pillow basalts from Rheinisches Schiefergebirge (Germany), Frankenwald, and Thüringer Wald within the Saxothuringian zone in Germany. These latter workers, in particular, emphasized the need for more research to reveal the ecological niche that cavities and amygdules in seafloor basalts could provide for life in volcanic rocks.

Chasmo- and cryptoendolithic microorganisms that inhabit the margins, walls, and pore spaces of fluid-filled cavities, voids, veins, and fractures of basaltic rocks can become fossilized via the precipitation of authigenic minerals, such as carbonates, clays, minerals, and zeolites (*e.g.*, Ivarsson *et al.*, 2008; Peckmann *et al.*, 2008). In this study, we present the results of a detailed investigation of objects with microorganism-like morphologies that occur within phillipsite-filled amygdules located at and near the outer surfaces of pillow basalts recovered from the Coral Patch Seamount in the eastern North Atlantic Ocean (Fig. 1); the preliminary findings related to this research were included in Cavalazzi *et al.* (2008). The combination of different methods of sample preparation and analytical techniques, which include optical and electron microscopy, confocal laser scanning microscopy, and Raman microscopy, permitted the investigation of two types of putative microbial structures and their associated chemical compositions. Our study provides additional evidence that vesicular basalt can support microbial ecosystems and that such communities may leave traces in the geological record. Of relevance to paleobiology and astrobiology search strategies is the likelihood that vesicular basalts with similar types of microenvironments would have been common on any wet (or formally wet) rocky planet that experienced extrusive volcanism throughout its geological history.

2. Materials and Geological Setting

The sample, a fragment ($\sim 90 \times 60 \times 40$ cm) of dark-reddish pillow basalt partially encrusted by fossiliferous pelagic limestone, was collected (August/September) during the scientific cruise SWIM 2004 (principal investigator: N. Zitellini, ISMAR-CNR, Bologna) of the R/V URANIA in the Gulf of Cadiz, eastern North Atlantic Ocean (Fig. 1). It was dredged from station SWIM04-29 (34°58.310 N to 34°56.773, 11°57.323 W to 11°57.140) on the flank of Coral Patch Seamount in the Ampère–Coral Patch Seamounts region from moderate depths (1018 m) (star in Fig. 1 shows approximate locality). Cores (2 cm in diameter) were drilled from the outer rind of the pillow basalt for this study.

The Ampère–Coral Patch Seamounts (31 Ma old) represent the intermediate phases of a ≥72 Ma old hot spot (Geldmacher and Hoernle, 2000), which also formed the

Ormonde, Unicorn, Seine, and Porto Santo Seamounts (Fig. 1). Located 460 km SW of the Ampère–Coral Patch Seamounts region, the Madeira Archipelago is the present location of the Madeira hot spot track. The Serra de Monchique Complex (72–70 Ma old alkaline volcanic rocks) in southern Portugal represents the vestiges of the early activity of the hot spot (Fig. 1). Geldmacher and Hoernle (2000) interpreted the alkaline volcanic rocks along the Madeira hot spot track, including the Ampère–Coral Patch Seamounts region, as resulting from the progressive melting and exhaustion of recycled (hydrothermally altered) basaltic oceanic crust in a discrete pulse of plume material as it upwelled and spread out at the base of the lithosphere. The composition of the basaltic rocks along the hot spot track evolves from transitional tholeiites to basanites to hawaiites to trachytes. The crustal oceanic rocks at Ampère–Coral Patch Seamounts form part of an alkali (hawaiite type) basaltic suite (Geldmacher and Hoernle, 2000).

3. Methods

The pillow basalt was subsampled and characterized initially by optical microscopy. Six subsamples drilled from the 2 cm diameter cores were analyzed for this study. For each subsample, one or two uncovered polished petrographic thin sections (30 μm thick) were prepared. Thin sections were investigated with the use of a transmitted optical light microscope, an Olympus BX51 TH-200 equipped with an Olympus DP12 digital microscope camera, and an Olympus BX51 TRF equipped with an Olympus DP72 digital microscope camera. Subsequently, the thin sections were examined with a confocal laser scanning microscope (CLSM) and a confocal Raman microscope.

Confocal laser scanning microscope images, obtained with a LSM 510/3 META microscope, provided a means to correlate features observed in the petrographic thin sections with native fluorescence found in the material. CLSM optical micrographs, acquired with the use of a Type FF fluorescence-free microscopy immersion oil, were recorded with CarlZeiss LSM Image Browser software. The image size was set at 512×512 pixels, and the area captured in each image measured $0.28 \times 0.28\ \mu m^2$. The images were recorded with the software operating in line mode, and four scanned images were averaged to reduce background noise. The CLSM images were acquired and stored as an electronic signal, which allowed us to apply several electronic image enhancement methods (Amos and White, 2003). Native fluorescence (488 nm excitation filter, 505 nm long-pass emission filter) produced by the sample was captured digitally in images acquired with the use of a plan-Apochromat 63× oil objective lens (numerical aperture = 1.4). Sequential images were recorded as 18 to 64 optical slices. Details about individual image acquisition parameters are provided (*e.g.*, in caption for Fig. 5). In general, slices 0.30 μm thick were acquired, and the stack size was defined as a function of the resolution required for any one image and corresponding thickness of the scanned volume.

Raman analyses and compositional maps were acquired with an alpha500 WiTec AFM-confocal Raman microscope. Three objectives (Nikon 20×, 50×, and 100×) and a frequency doubled Nd:YAG (532 nm) Ar-ion 20 mW monochromatic laser source were used to collect the Raman spectra. Beam centering and Raman spectra calibration were performed before spectra acquisition by using a Si standard with a characteristic Si Raman peak at 520.4 cm^{-1}. The optimum power for *in situ* analyses of different minerals, between 1.67 and 1.70 nW at the sample surface, was determined experimentally. The Raman spectra and maps were collected a few micrometers below the surface of any one specimen to eliminate possible contamination that might have resulted from the preparation and handling of the thin sections. Raman analyses and maps were recorded and treated with WITecProject2.00 software. For final analysis, the thin sections that were uncontaminated with oil were cut into subsections, etched in an aqueous solution of 1% HCl for 10 s (to remove any room contamination and hand oils), and then air dried. The thin section pieces were mounted on aluminum stubs covered with carbon-conductive adhesive tape.

Au-coated, C-coated, and non-coated thin sections were observed with an environmental scanning electron microscope (ESEM), FEI Quanta 200, equipped with an Oxford Instruments INCA 350 X-ray energy-dispersive spectrometer (EDS) system, and a Hitachi S4200 field emission gun scanning electron microscope (FEG-SEM), equipped with Si (Li) detectors from Oxford Instruments Link ISIS. A conductive (Ag) paint was spread sparingly around the perimeter of the uncoated sample prior to scanning electron microscope (SEM) analysis to reduce surface charging. Energy-dispersive X-ray (EDX) analyses were qualitative and semi-quantitative. ESEM observations were conducted in high and low (1 and 0.5 torr) vacuum. The operating conditions of the scanning electron microscopes were 5–25 keV accelerating voltage for imaging and 5–15 keV for elemental analyses. All the instruments used in this study are located at the Department of Geology, University of Johannesburg (South Africa); at the Centre de Biophysique Moléculaire, CNRS-Orléans (France); at the Centre de Microscopie Electronique, Université d'Orléans (France); and at the Centro Interdipartimentale Grandi Strumenti, Università di Modena (Italy).

4. Results

4.1. Rock textures

The Coral Patch Seamount pillow basalt is characterized by a vesicular (~15–20% vesicles) glass rind that contains numerous cooling fractures (*i.e.*, quenched during degassing due to rapid chilling) (Fig. 2). The glassy rind has experienced extensive palagonitization, a process that involves low-temperature hydrolitic alteration of mafic glass by seawater (Stroncik and Schmincke, 2001). As a result of this process, the glass devitrifies to microcrystalline secondary minerals as the sample ages. In thin section, the palagonite mainly consists of extremely fine-grained reddish-brown secondary minerals (Fig. 2). Rare fractured olivine (forsterite) relicts and phenocrysts (≤500 μm in diameter) of clinopyroxene (augite) and chromian spinel (magnesiochromite) occur throughout the glassy rind (Fig. 2; Table 1).

The vesicular texture occurs along the outer margin of the glassy rind of the pillow basalt. It consists of subspherical to elongate vesicles characterized by a diameter from 200 to 300 μm to less than 1.5 mm (Fig. 2). The vesicles are partially to totally filled by transparent to translucent zeolite (K-phillipsite) (Fig. 2; Table 2). Mineral-filled vesicles are

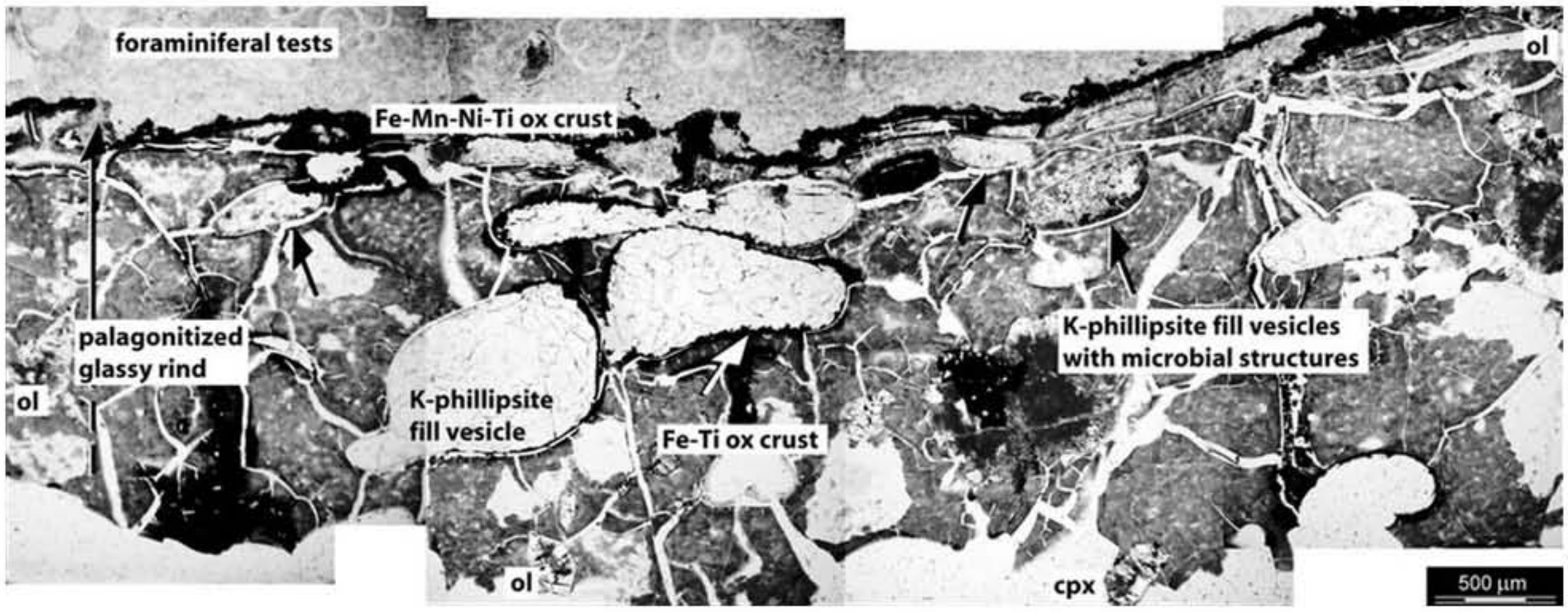

FIG. 2. Mosaic of transmitted-light photomicrographs of a petrographic thin section of the vesicular basalt. The palagonitized, reddish-brown glassy rind of the pillow basalt is characterized by amygdules, that is, partially or totally infilled by K-phillipsite, sparse grains of altered phenocrysts of olivine (ol) and clinopyroxene (cpx), and cooling fractures. Some amygdules (black arrows) are filled by granular K-phillipsite with disseminated Fe-Ti oxides and microbial-like structures. A Fe-Mn-Ni-Ti-oxide crust separates the outer edge of the pillow basalt from the encrusting foraminifera-rich lithified pelagic ooze and K-phillipsite.

referred to as amygdules. Some amygdules are filled with elongate fibrous K-phillipsite crystals that are radially arranged and protrude away from discrete nucleation centers located along the vesicle walls. Other K-phillipsite–filled amygdules display a granular texture (Figs. 2 and 3A).

The surface of the pillow basalt is characterized by either a 100–150 μm thick reddish-black crust of Mn-Fe-Ti-Ni-enriched oxides or a crust of lithified Ca-carbonate ooze that originally contained abundant microfossils such as calcareous nannoplankton and planktonic foraminiferal tests (Fig. 2). Although difficult to distinguish in thin section, fossils of calcareous nannoplankton (rare specimens of *Sphenolithus* spp. and *Cyclicargolithus* spp.) were identified in the carbonate. Rare fragments of radiolarians occur among the abundant remains of foraminifera. The planktonic foraminiferal assemblage is dominated by epi- and mesopelagic genera, such as *Globigerina, Globigerinoides, Globorotalia, Globoturborotalia,* and *Orbulina*.

4.2. Microbe-like morphologies

Possible biogenic filamentous and spherical structures and small grains of Ti-Fe oxides (anatase) were found in the K-phillipsite–filled amygdules that display a granular texture and are located closest to the outer margin of the pillow basalt (Fig. 3; Table 2). The orange-red microbe-like structures appear diffuse and transparent when viewed with plane polarized light, as shown in the petrographic thin section photomicrographs of Figs. 4–10.

4.2.1. Filamentous structures. The filamentous structures appear as isolated objects that are characterized by a constant diameter of 2.5–3.5 μm and an observed maximum length of 30 μm (Fig. 4). Enclosed in a granular K-phillipsite matrix, the filamentous structures have a sinuous to straight morphology with a smooth surface (Fig. 4A), although the outer surface of some rare specimens, such as the ones

TABLE 1. RAMAN DETECTION OF RARE RELICT CRYSTALS WITHIN THE GLASS RIND

Raman spectra

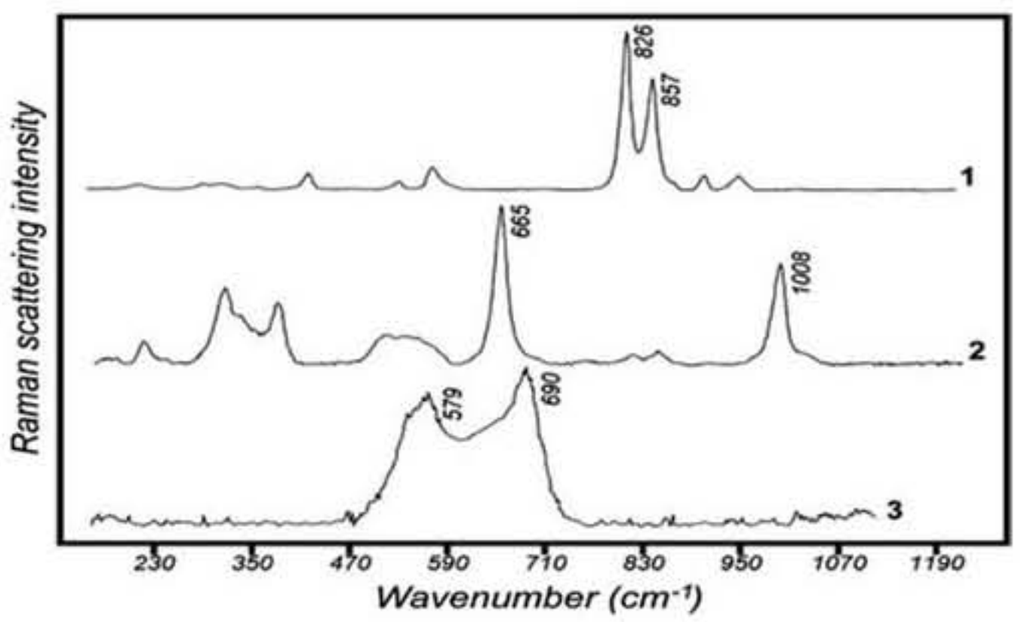

Raman spectrum 1: measured spectrum (532 nm) of olivine, forsterite (Mg_2SiO_4). Reference spectrum: forsterite (532 nm), RRUFF ID: R040018.
Raman spectrum 2: measured spectrum (532 nm) of clinopyroxene, augite ($(Ca,Mg,Fe)_2(Si,Al)_2O_6$). Reference spectrum: augite (532 nm), RRUFF ID: R061086.
Raman spectrum 3: measured spectrum (532 nm) of chromium spinel, magnesiochromite ($MgCr_2O_4$). Reference spectrum: magnesiochromite (532 nm), RRUFF ID: R060796.

All peaks in the region considered for each spectrum represent their vibrational mode. Raman spectra were calibrated with reference spectra after RRUFF DataBase (Laetsch and Downs, 2006).

TABLE 2. THE MINERAL PHASES ANALYZED BY SEM-EDX MICROANALYSIS AND RAMAN MICROSCOPY OF THE AMYGDULES FROM THE GLASSY PILLOW BASALT FRONT

SEM-EDX microanalyses: K-phillipsite

Samples	SiO_2	Al_2O_3	FeO	MgO	CaO	Na_2O	K_2O	*Total*
CPR 01.1	61.45	23.94	—	0.33	0.00	5.13	9.16	100.01
CPR 01.2	59.44	24.48	—	0.71	0.23	6.69	8.45	100.00
CPR 01.3	61.22	22.77	—	0.87	1.12	5.70	8.18	100.01
CPR 02.1	59.52	23.24	—	0.31	0.26	6.60	10.07	100.00
CPR 02.3	60.44	22.56	0.56	0.86	1.85	5.43	8.29	99.99

Phillipsite: $(Ca,Na_2,K_2)_3(Al_6Si_{10})O_{32}12H_2O$.
Analyses were made on C-coated thin section using 15 keV accelerating voltage.

Raman spectrum: K-phillipsite

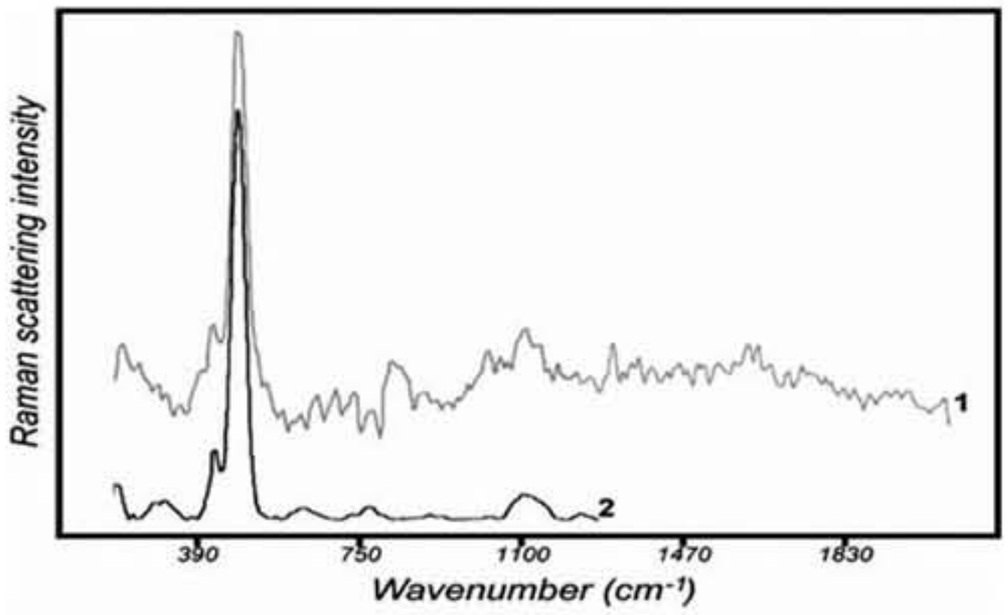

Raman spectrum 1*: measured spectrum (532 nm) of mineral phase, phillipsite, filling vesicles.
Raman spectrum 2: reference spectrum of phillipsite (532 nm) (RRUFF ID: R060161).

SEM-EDX spectrum: K-phillipsite

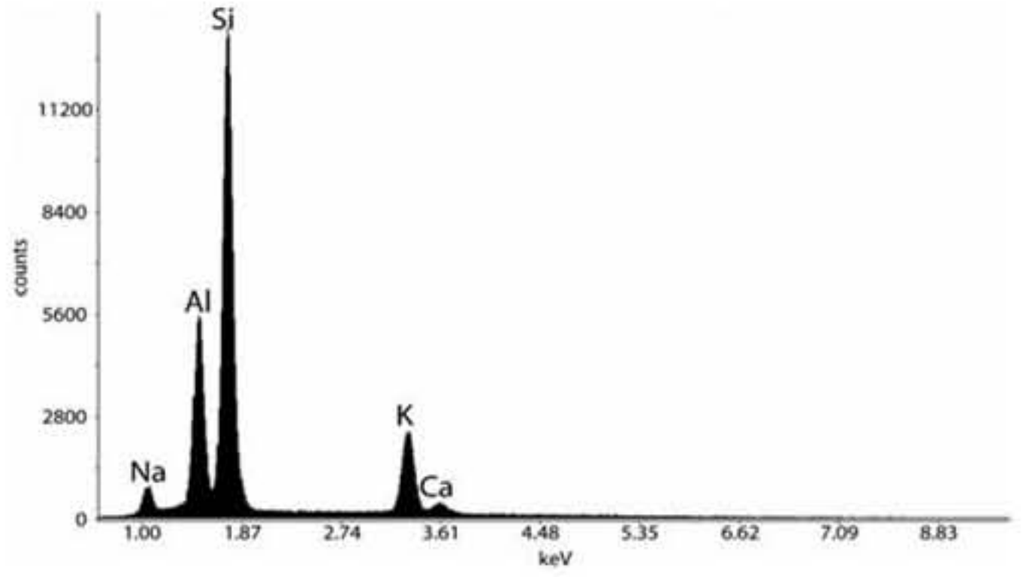

SEM-EDX spectrum: spectrum was acquired on C-coated thin section using 15 keV accelerating voltage.

Raman spectrum: anatase

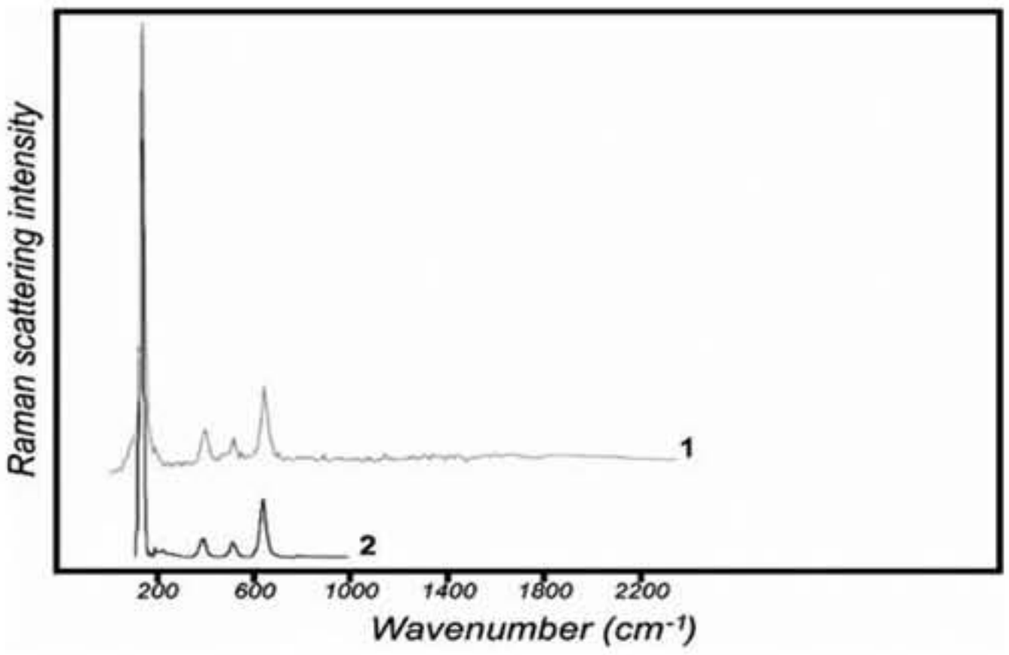

Raman spectrum 1*: measured spectrum (532 nm) of mineral phase, anatase (TiO_2), associated to K-phillipsite filling vesicles.
Raman spectrum 2: reference spectrum of anatase (532 nm) (RRUFF ID:R070582).

*All peaks in the region considered for the spectrum represent the vibrational mode.

shown in Fig. 4B, appear undulated. Because the vesicle walls are often incrusted with Fe-Ti oxides (Figs. 2 and 3), only a few sinuous filamentous structures with a smooth surface are observed to be attached with one end to the vesicle walls (white arrow in Fig. 4C). The filamentous structures—filled with K-phillipsite—consist either of individual tubular forms or short chains of small spheres (~3–2.5 μm in diameter) (Figs. 5 and 6). Both types of filamentous structures are characterized by a distinctive native fluorescence (Fig. 5). Some of the tubular structures are encapsulated in an amorphous C-Fe-O-rich envelope less then 500 nm thick (black arrows in Fig. 6B, 6E).

Raman analyses were made of some of the objects that display a filamentous morphology (Fig. 7). Raman mapping (Fig. 7C–7E) provides a means with which to correlate the objects with cellular-like morphologies and their mineralogical composition. The filaments consist of K-phillipsite (Fig. 7A–C), whereas the amorphous envelope around some of the filamentous structures consists of Fe oxyhydroxide, lepidocrocite that is enriched in carbonaceous matter (Fig. 7A–B, 7D–E). In Fig. 7B, the Raman spectrum 2 includes the major bands of the first-order region of the disordered carbonaceous matter (D1: ~1345 cm^{-1}; G1: ~1600 cm^{-1}) associated with the filamentous morphologies. The relative intensity of

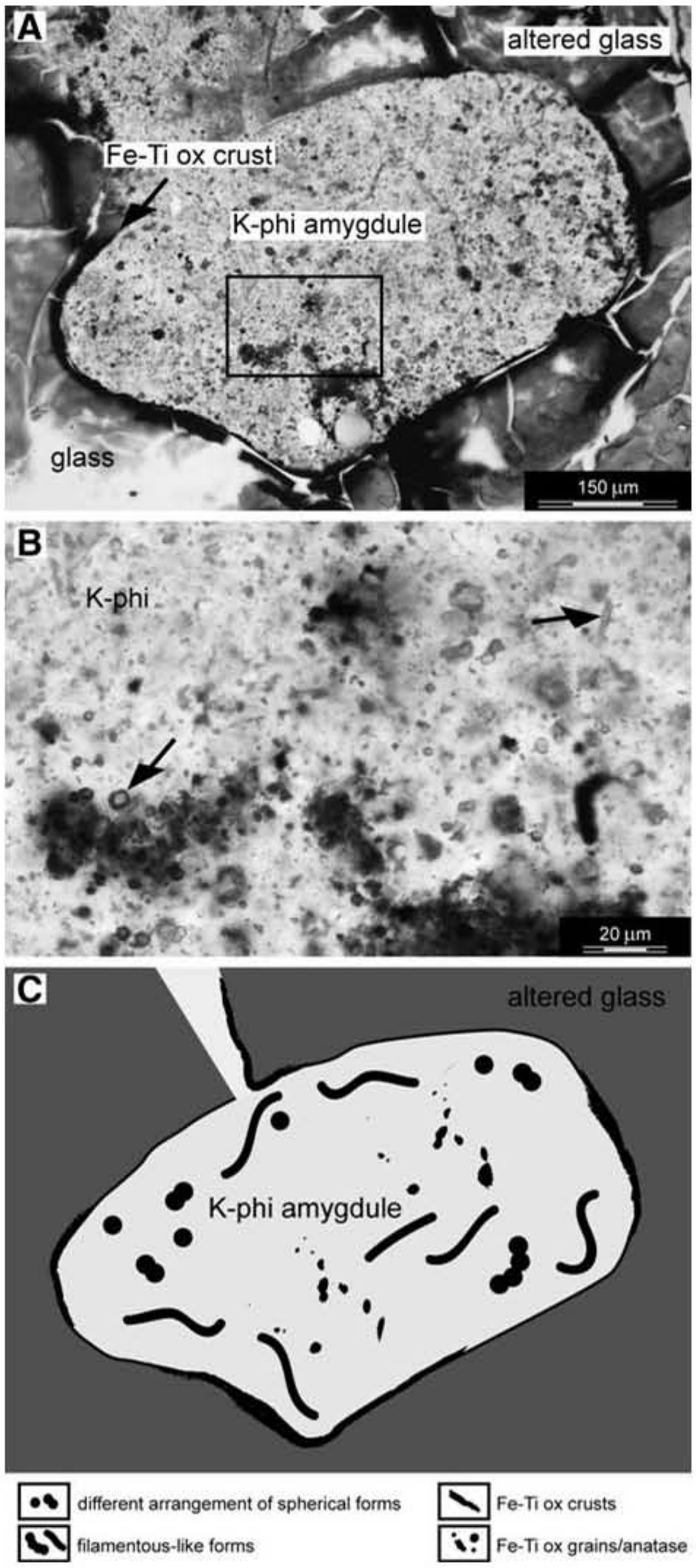

FIG. 3. Thin section transmitted-light photomicrograph of an amygdule from the altered glass of pillow basalt rinds (**A**). (**B**) Illustrates detail of the boxed area in (A) and shows the distribution of spherical and filamentous structures (black arrows). (**C**) Simplified sketch of an amygdule that illustrates their dominant characteristics and distribution of purported microfossils. Details in (C) are not to scale. K-phi, K-phillipsite.

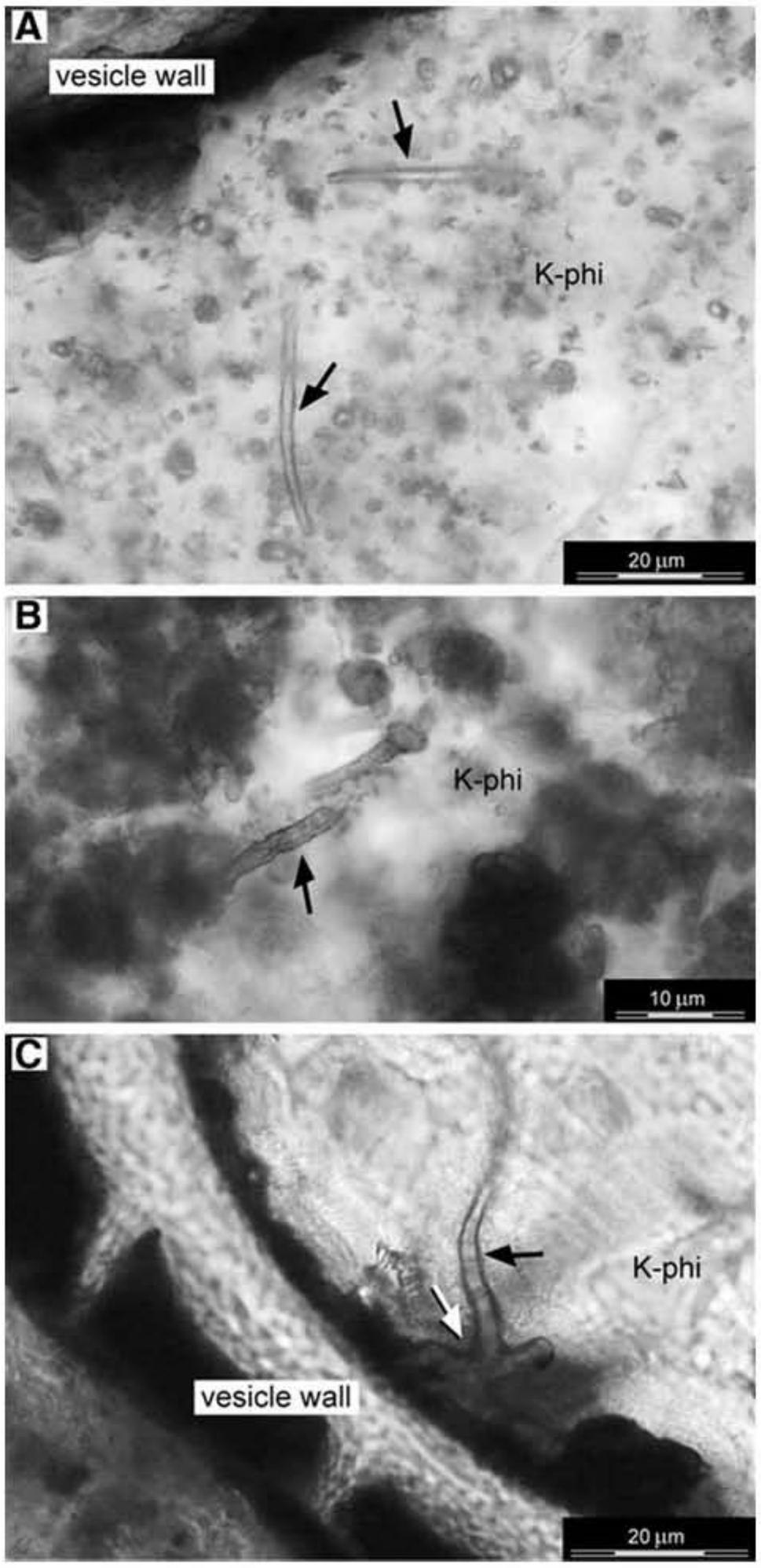

FIG. 4. Thin section transmitted-light photomicrographs that reveal the presence of individual filamentous structures (diameter size: 2.5–3.5 μm) within K-phillipsite–filled vesicles. The filamentous structures show smooth sinuous [black arrows in (**A**) and (**C**)] and corrugated [arrow in (**B**)] morphologies. In (C), (white arrows) a filament structure is attached to the vesicle wall and embedded in K-phillipsite. K-phi, K-phillipsite.

the D1 and G1 bands indicates a poorly crystalline, disordered carbonaceous matter.

4.2.2. Spherical structures. Two sizes of spherical structures were observed: macrospheres, with an average outer diameter of 4 μm, and smaller microspheres, with an outer diameter between 2 and 2.5 μm (Fig. 8). The outer walls of the macrospheres display a reddish, transparent appearance in petrographic thin section. The macrospheres occur mainly as paired bodies or as aggregates (Fig. 8A–B). The microspheres also appear in petrographic thin section as transparent, smooth-surfaced individuals or paired bodies (Fig. 8C). SEM-EDX analysis revealed that the distinctive outer rims of the macrospheres and microspheres have a similar composition that shows an enrichment of carbon, Ti, and Fe

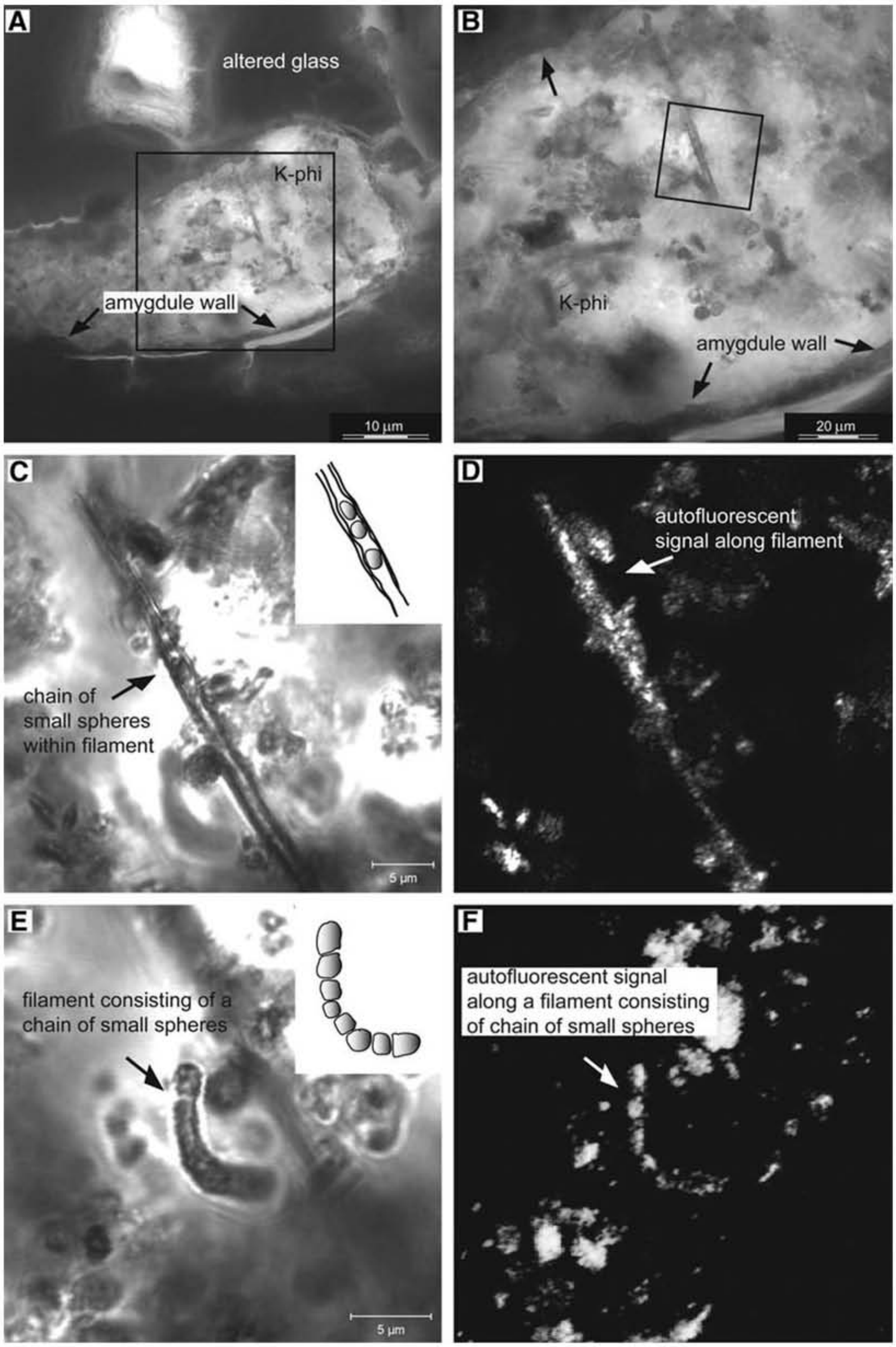

FIG. 5. Magnified view of optical transmitted-light (**A–B**) and CLSM images (**C–F**) of putative microfossils, which include filamentous structures and short chains of small spheres embedded in the K-phillipsite–filled vesicles. The CLSM images provide details of the structures observed in the boxed area shown in (B). The CLSM images reveal a native florescent signal associated with the filamentous structures, highlighting the internal fine-scale morphological features, which include small spheres. CLSM acquisition parameters: (C) image from stack scan mode (stack size/μm: $35.7\times35.7\times5.1$ μm^3; stack size/pixel: $512\times512\times18$; pixel depth: 8 bit; scaling: $x=0.070$ μm, $y=0.070$ μm, $z=0.30$ μm; wavelength: 488 nm 9.0%); (D) image from plane scan mode (stack size/pixel: $1\times1\times1$; pixel depth: 8 bit) obtained from (C); (E) image from stack scan mode (stack size: $27.3\times27.3\times5.1$ μm^3; stack size/pixel: $512\times512\times18$; pixel depth: 8 bit; scaling: $x=0.053$ μm, $y=0.053$ μm, $z=0.30$ μm; wavelength: 488 nm 9.0%); (F) image from plane scan mode (stack size/pixel: $1\times1\times1$; pixel depth: 8 bit) obtained from (E). K-phi, K-phillipsite.

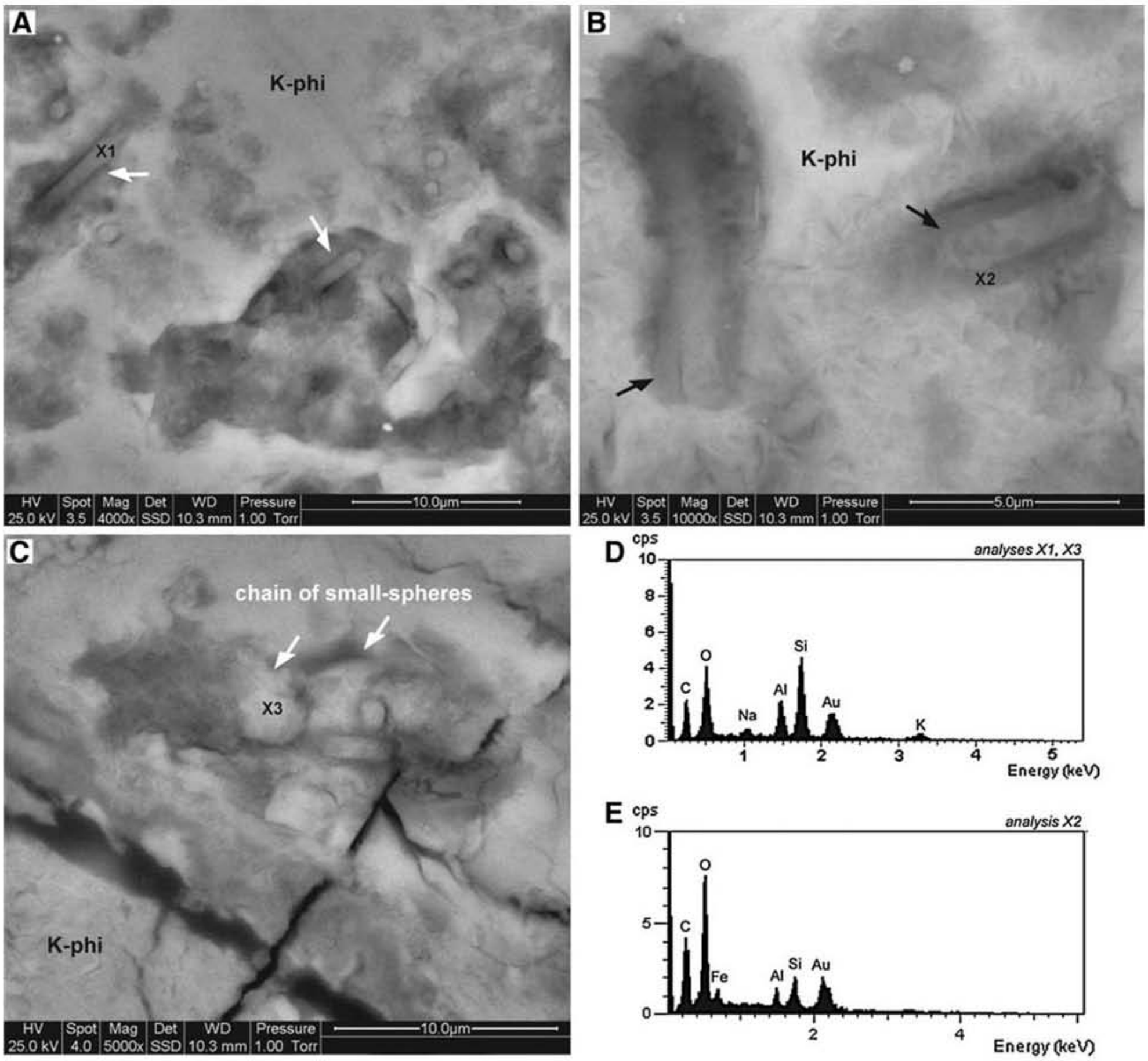

FIG. 6. ESEM images of filamentous morphotypes within K-phillipsite–filled vesicles. The filamentous structures consist of K-phillipsite microtubes [X1: EDX spectrum in (**D**); white arrows in (**A**)] surrounded by an Fe-rich carbonaceous membrane-like envelope [X2: EDX spectrum in (**E**); black arrows in (**B**)]. Some filaments are formed by short chains of small spheres [X3: EDX spectrum in (**D**); white arrows in (**C**)]. The ESEM images were acquired on uncoated and lightly etched (HCl 1%, less than 4 s) thin sections in low vacuum (1 torr) with a 25 keV electron beam. The samples were subsequently Au-coated for ESEM-EDX analyses. EDX data were acquired with a 5 keV accelerating voltage. K-phi, K-phillipsite.

relative to the matrix (Fig. 9). Raman microscopy revealed that the Ti-enriched phase is anatase (TiO_2) (Table 2) and that it is associated with carbonaceous matter (Fig. 10).

5. Discussion

We infer the biogenicity of the filamentous and spherical structures in the K-phillipsite amygdules from the Coral Patch Seamount pillow basalt based on the full suite of morphological, mineralogical, and chemical characteristics that were observed with different analytical instruments over a range of scales from the microscopic to submicroscopic (*cf.* Buick, 1990; Knoll, 1999; Summons *et al.*, 1999; Cady *et al.*, 2003; Brasier *et al.*, 2006; Schopf *et al.*, 2007, 2010a). Although the morphology alone of bacteria-like objects may not be a diagnostic biosignature, it serves an important role in spatially locating within a potential ecological niche candidate biosignatures that should be characterized chemically in more detail. The discovery of a suite of possible biosignatures associated with the morphological objects strengthens our interpretation of their biogenic origin.

In summary, the suite of possible biosignatures that are consistent with a biogenic origin for the microbe-like remains includes the following:

(1) Morphology—distinctive micrometer-sized objects that display sizes, size distributions, and filamentous and spherical morphologies consistent for bacteria;

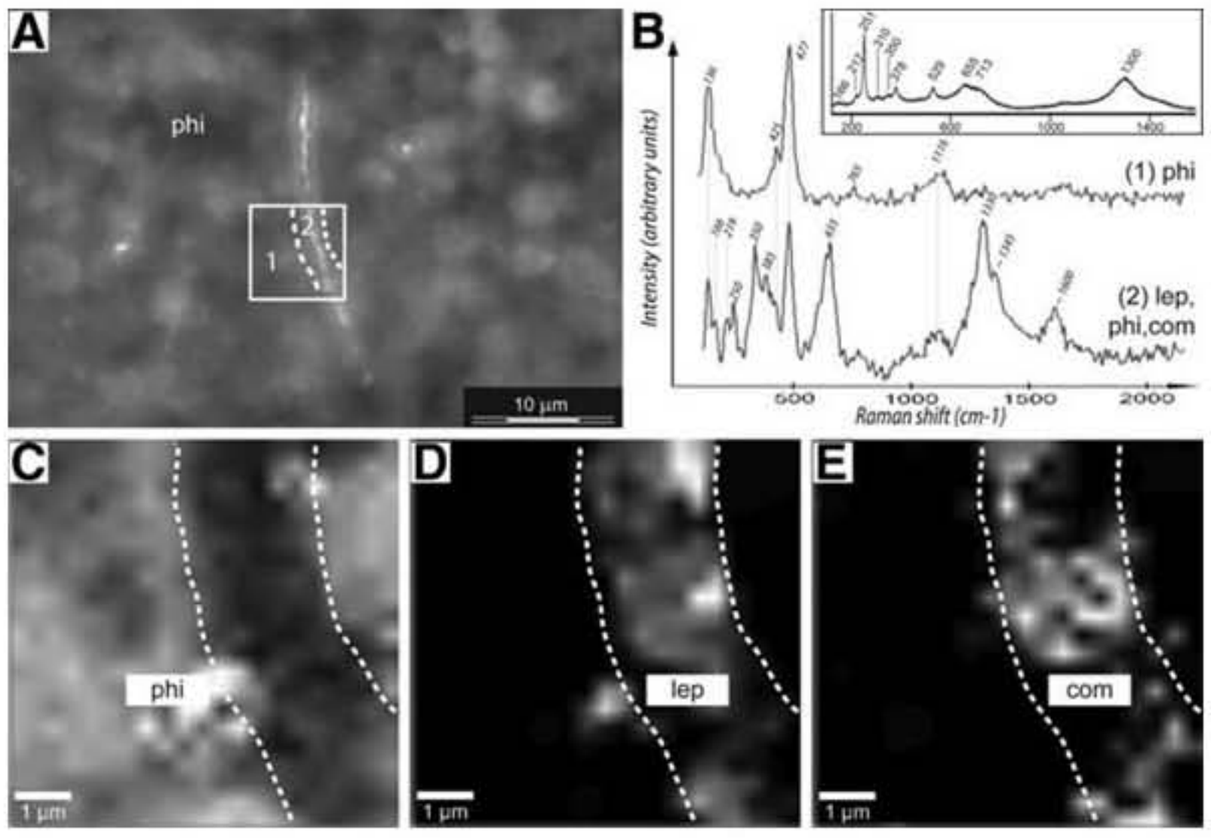

FIG. 7. Optical photograph and Raman analyses of an area in a polished thin section that contains a filament. (**A**) Reflected light optical photomicrograph (focus plane: 7 μm below to the surface). The number indicates the location from which the representative Raman spectra of the host matrix and filamentous structure (dashed lines) were collected, whereas the boxed area indicates the location of the Raman maps. (**B**) The host matrix, spectrum 1, consists of phillipsite, and the filamentous structure as shown in the multiphase spectra 2 is made of lepidocrocite (lep) associated with phillipsite (phi) and traces of carbonaceous matter (com). Raman spectra were calibrated after RRUFF DataBase (Laetsch and Downs, 2006), Demoulin *et al.* (2010), and Marshall *et al.* (2010). Inset shows the reference spectrum of pure lepidocrocite (532 nm) after Demoulin *et al.* (2010); see also reference spectrum (780 nm) RRUFF ID R050454. (**C–E**) Raman maps that show the distribution of phillipsite (phi), lepidocrocite (lep), and carbonaceous matter (com) of the area that contains the filamentous structures (dashed lines). Data are presented as a black-white intensity ratio map where white regions indicate high concentrations of the component labeled at the bottom of each panel. The Raman maps correspond to the same focal plane imaged in (A).

(2) Chemical composition—carbonaceous composition of microbial-like morphological features and a correlation of the carbonaceous remains and authigenic mineral precipitates associated with the purported microfossils, which are consistent for bacteria;
(3) Ecological setting—habitat for microbial communities with enhanced preservation potential.

5.1. Morphology of putative microfossils consistent with life

Though morphology alone cannot serve as a definitive biosignature (*e.g.*, García Ruiz *et al.*, 2002), morphological evidence of microfossil-like objects helps to focus the search for additional possible biosignatures from such structures (Cady *et al.*, 2003). The purported microfossils in the basalt amygdules studied here display a number of key morphological attributes that are consistent with a biological origin: (i) size distribution typical of filamentous and coccoidal prokaryotes; (ii) minimal size variation within any one particular morphological group (filaments display diameters 2.5–3 μm, Fig. 4; macrospheres ~4 μm, and microspheres 2–2.5 μm, Fig. 8); (iii) shape consistency (*e.g.*, filamentous and spherical) with constant diameters (Figs. 4–10); and (iv) an arrangement and structural complexity of individual cells or colonial aggregates (*e.g.*, short chains of small spheres that comprise filaments, Figs. 5 and 6). The lack of variation in the morphological attributes is much more typical of microbial

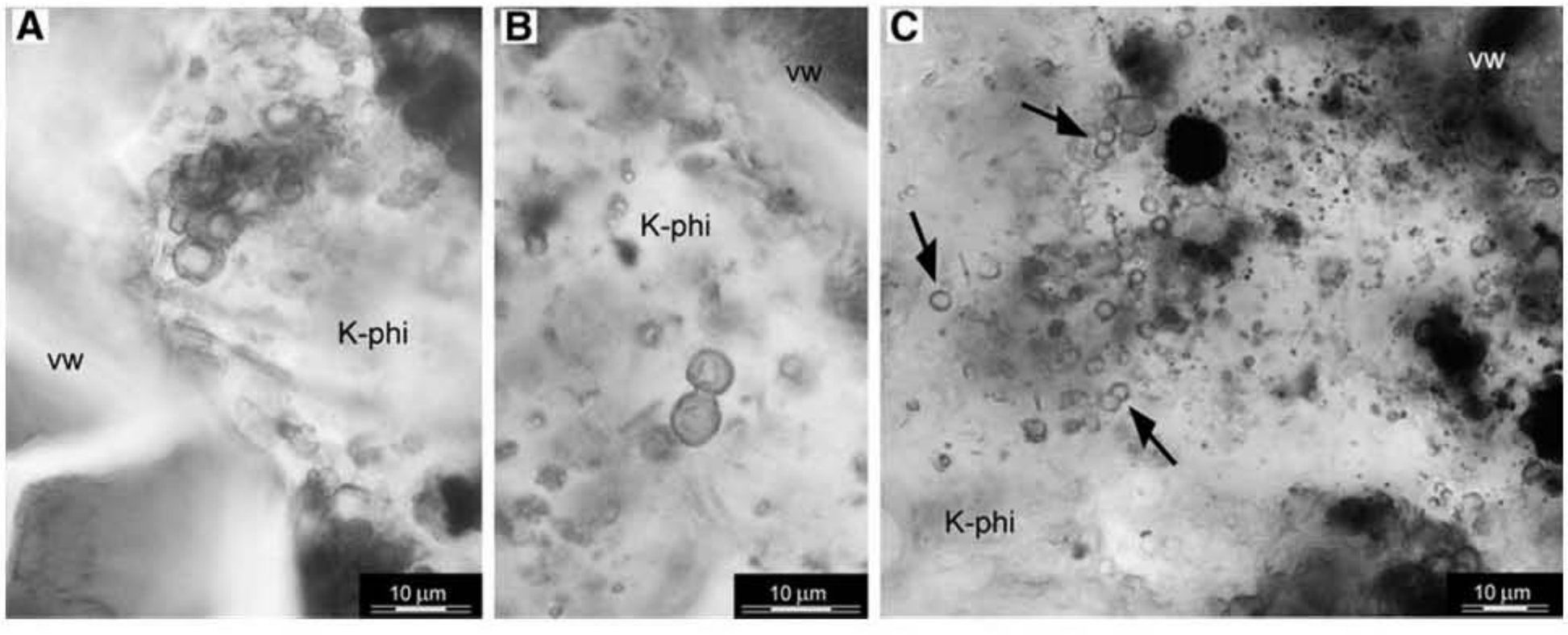

FIG. 8. Transmitted light photomicrographs of a petrographic thin section that illustrates two sizes of spherical structures within the K-phillipsite–filled vesicles. (**A**, **B**) The reddish-brown macrospheres (~4.5 μm outer diameter) appear as thick-walled semi-spheroids. (**C**) The transparent (~3 μm diameter) microspheres occur as isolated or paired bodies (black arrows). K-phi, K-phillipsite; vw, vesicle wall.

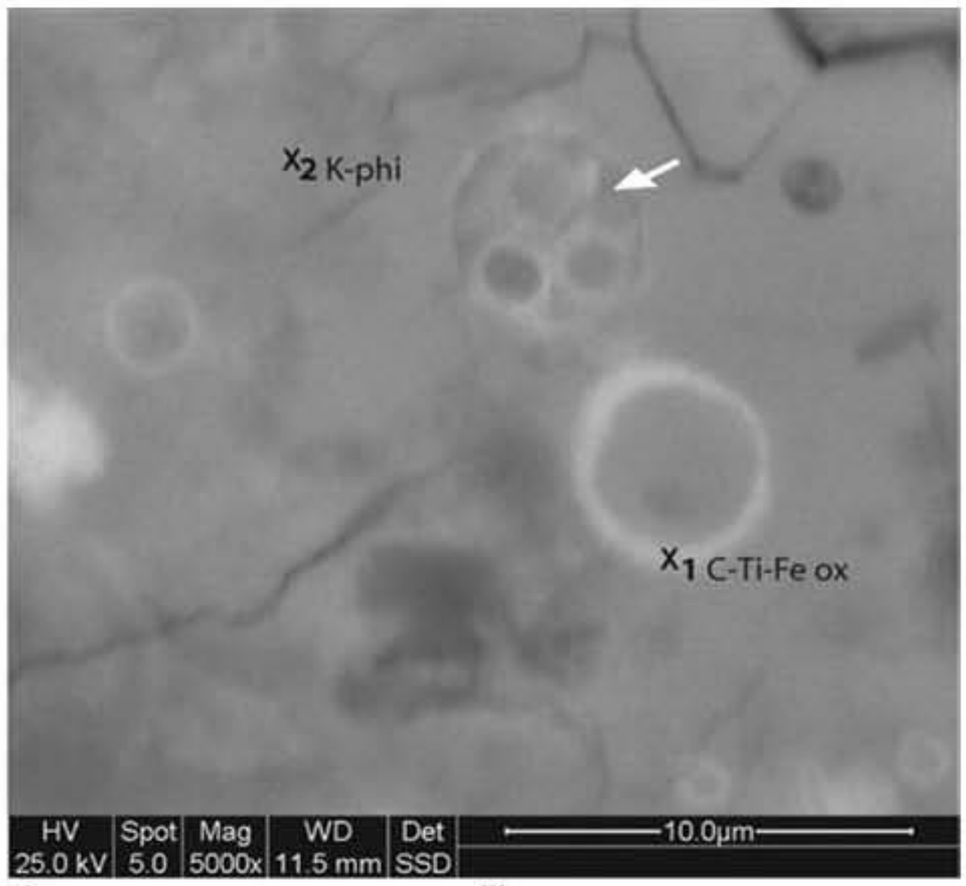

FIG. 9. ESEM image of spherical structures and their chemical composition. They appear as circular structures with an outer rim of C-rich Ti-Fe oxides (EDX spectra). Some of these structures are filled by smaller spheres (arrow) that are similar in composition. The structures were imaged on uncoated samples, and the two spectra (x_1: spherical structure; x_2: host matrix) were acquired with 5 keV accelerating voltage on a Au-coated sample. K-phi, K-phillipsite; ox, oxide.

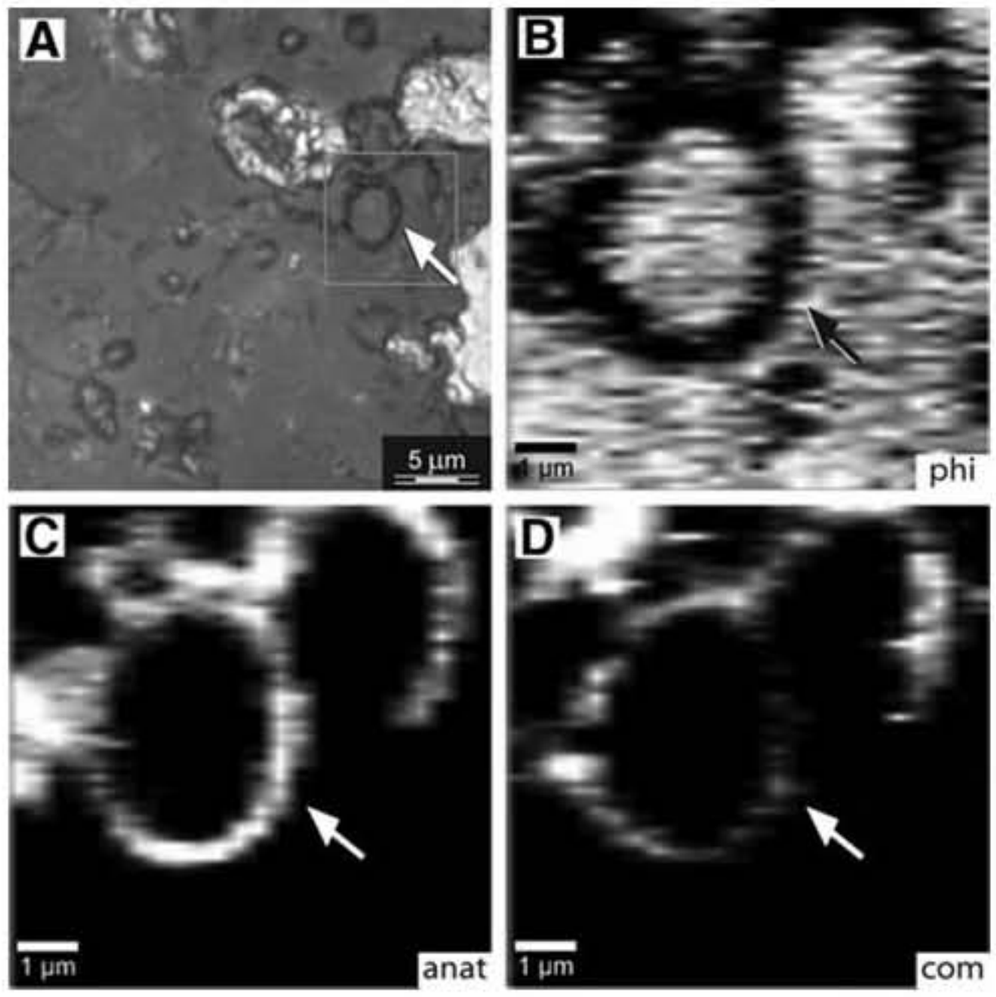

FIG. 10. Optical photograph and Raman maps of the area containing spherical structures in a polished thin section. (**A**) Reflected light optical photograph (focus plane: 5 μm below to the surface) of the spherical structures ($\sim$4 μm diameter). The boxed area indicates the location of the Raman maps. (**B–D**) Raman maps reveal the distribution of phillipsite (phi), anatase (anat), and carbonaceous matter (com), which generate negative and positive ring shape structures, respectively. The data are presented as a black-white intensity ratio map where white regions indicate the presence of the component labeled at the bottom of each panel. The Raman maps correspond to the focal plane imaged in (A). Arrows locate walled spheres in the different panels.

assemblages than it is of similar abiotic structures (Brasier *et al.*, 2006).

Filamentous and spherical microorganisms are the most common type of micrometer-scale morphology found in basaltic subseafloor niches. Such microbial morphotypes colonize surfaces, fractures, and vesicles in volcanic rocks to obtain energy and nutrients from reduced chemical species released from basalt during dissolution/alteration, and they establish themselves in physically stable environments where they can proliferate and, when necessary, escape predation (*e.g.*, Edwards *et al.*, 2004, 2005; Cockell and Herrera, 2008; Santelli *et al.*, 2008; Chan *et al.*, 2011). Older filamentous and spherical microfossils have been found in association with filled fractures and vesicles in basaltic volcanic rocks (*e.g.*, Ivarsson *et al.*, 2008; Peckmann *et al.*, 2008).

5.2. Chemical composition of putative microfossils indicative of microbial life

The chemical characteristics of the purported microfossils are consistent with a biogenic origin. Noteworthy is the correlative nature of the carbonaceous material and native fluorescence produced by many of the purported microfossils (Figs. 5 and 6). Carbon enrichment and carbonaceous matter were observed in both the filaments and coccoidal structures relative to the mineral matrix in which they are embedded (Figs. 6, 7, 9, 10). The relatively low abundance of carbon in the mineral matrix of igneous rocks has led to its use as a biosignature in this type of environmental setting when there is a relative enrichment in its concentration and an association with microbial-like structures (Furnes *et al.*, 2002; Banerjee and Muehlenbachs, 2003; Ivarsson *et al.*, 2008).

Laser Raman microscopy has been successfully used to characterize natural carbonaceous compounds (*e.g.*, Jehlinča and Bény, 1992; Marshall *et al.*, 2010) and for chemical imagery of microfossils (Schopf *et al.*, 2005, 2006, 2010a, 2010b). Here, we were able to confirm the intimate association of disordered carbonaceous material with the candidate biosignatures, using *in situ* Raman mapping. In this study, native fluorescence of the microfossil-like objects in the basalt amygdules was observed with a CLSM (488 nm excitation and 505 nm emission wavelengths). Native fluorescence of bacteria-like structures in the crevices of natural basalt samples has been detected with deep-UV (<250 nm excitation wavelength) laser-induced fluorescence and used as a near real-time optical imaging method (Bhartia *et al.*, 2010). The co-occurrence of biomolecules, native fluorescence, and (living and fossil) microbial morphotypes has been demonstrated with different (*e.g.*, <250 and 488 nm) CLSM excitation wavelengths in several natural environments (*e.g.*, Amos and White, 2003; Schopf *et al.*, 2006, 2010a; Bhartia *et al.*, 2008, 2010; Santelli *et al.*, 2008). Of most interest here is a study in which *in situ* native fluorescence and resonance Raman

spectroscopy were coupled with other analytical techniques such as environmental scanning electron microscopy–energy-dispersive X-ray spectroscopy to detect microorganisms on the rim of small spherical cavities (vesicles) within volcanic glass (Fisk *et al.*, 2003). For instance, the *in situ* multiple analytical techniques used in this study permit the identification of similar clay-covered spherical forms. In both cases, the detected morphological forms resemble known deep-sea microorganisms.

Native fluorescence of the lepidocrocite-rich areas that surround the filamentous structures (Fig. 6B) indicates the presence of organic remains in the type of occurrence expected when the extracellular polymeric substances of sheathed microorganisms are mineralized (*e.g.*, Bhartia *et al.*, 2010). Sheathed Fe-oxidizing microorganisms (van Veen *et al.*, 1978; Emerson and Moyer, 1997; Chan *et al.*, 2011) are characterized by chains of cells that, when encased in their tubular sheaths, appear as filaments (*e.g.*, note the short chains of sphere observed in Fig. 5C–F).Though it is possible that all the native fluorescence associated with the morphological remains of the purported microfossils is produced by small autofluorescent crystals, the nonbiological explanation (the "null hypothesis" *sensu* Brasier *et al.*, 2006) for the observed phenomenon is not favored because (i) the authigenic mineral precipitates (*e.g.*, lepidocrocite, Fe hydroxide, and anatase Ti oxide; see below) are not known to be autofluorescent at the excitation wavelengths used in this study and (ii) the native fluorescence is always correlated with microfossil-like morphologies.

Native fluorescence of minerals is related to the presence of impurities, organic activators, and the excitation wavelengths used (Gorobets and Rogojine, 2002). Although few data are available in the literature with regard to the potential to induce native fluorescence in minerals for the excitation wavelength used here (λ_{exc} = 488 nm), laser-induced fluorescence of the mineral phases associated with the bacteria morphologies [the natural Fe(III)-hydroxide and Ti-oxide mineral phases] are not known to fluoresce when excited with UV or visible radiation (Gaft *et al.*, 2005). Typically, lepidocrocite, γ-Fe(III)O(OH), cannot be the source of the luminescence because of the nature of it; the type and structure of this mineral render it impracticable for emission of luminescence by the mineral itself even with impurities in its structure. Lepidocrocite can form, however, with external macroscopically mixed luminescent impurities.

5.3. Chemical composition of authigenic minerals consistent with microbial life

The mineralogy of the authigenic precipitates, Fe and Ti metal oxides, associated with the purported microfossils is consistent with the activities of a microbial population associated with subseafloor environments. For example, the iron-oxide lepidocrocite precipitates when sheathed iron-oxidizing filamentous bacteria remove iron from solution (Emerson and Moyer, 2002). Though bacterial sheaths can provide a physically and chemically protective environment in which the cells can grow and divide, once mineralized they limit the diffusion of nutrients into cells. Microbial surfaces and extracellular polymeric substances are known to enhance the concentrations of certain elements, such as Fe and Ti, relative to the concentrations of these elements in the surrounding environment (Beveridge, 1989; Konhauser, 1998). High concentrations of Fe in the sheaths and on microorganisms in the seafloor environment are considered to result from active microbial interactions with the volcanic materials. In such processes, lithotrophic microorganisms utilize the redox potential of the volcanic minerals as a mechanism to obtain energy (Thorseth *et al.*, 2001; Bach and Edwards, 2003; Edwards *et al.*, 2005; Santelli *et al.*, 2008). Although several microfossils' structures are known to be preserved or contain mineral mixtures dominated by metal oxides, and the role of metabolism and biomineralization processes of Fe oxidizers are relatively well known (*e.g.*, Emerson and Moyer, 2002; Kappler and Straub, 2005), it is worth noting that, at present, the interactions between Ti and microorganisms and the role of Ti in microbial fossilization are poorly understood (Shabtai and Fleminger, 1994; Glamoclija *et al.*, 2009). Though some prokaryotes are known to adsorb TiO_2 during metabolic processes (Shabtai and Fleminger, 1994; Bedard *et al.*, 2006), the precipitation of titanium (and iron) oxide minerals is commonly thought to represent abiogenic low-temperature alteration of basaltic glass with seawater (*e.g.*, Stroncik and Schmincke, 2001). It was impossible in this study to establish whether the selective Ti mineralization of the spherical structures via anatase was a passive or microbially controlled fossilization process.

5.4. Timing of fossilization

Vesicles are primary segregation structures that represent the fossilized vestiges of degassing bubbles trapped during extrusion and decompression from a volatile-rich melt source (Peck, 1978). Although it is difficult to determine when the minerals infilled the vesicles, characteristics of the microhabitat and microfossil taphonomy provide some information with regard to the involvement of microorganisms in the process. Given their distribution within the K-phillipsite–filled amygdules, the microbial structures represent endolithic and, most likely, cryptoendolithic filamentous and spherical microorganisms. Unfortunately, because our microfossils were not associated with any multiple paragenetic sequences of cements (*e.g.*, Peckmann *et al.*, 2008), we were unable to determine precisely when the vesicles hosted life. The presence of the purported fossil microorganisms in amygdules in close proximity to the outer margin of the pillow basalt, along with the attachment of some of the microfossils to the walls of the vesicles (Fig. 4C) and the absence of granular or tubular alteration textures in the walls of the vesicles and glass shards, suggests that early precipitation of the phillipsite in the vesicles and pore space reduced the fluid circulation and inhibited the growth of euendolithic microorganisms (see Fisk *et al.*, 2003). The vesicular microhabitat would most likely have been a nutrient-rich micro-environment with the nutrients coming from alteration of the volcanic rocks. A circumneutral to alkaline (pH ≥ 7) fluid environment within the vesicles is indicated by the presence of abundant TiO_2 in the K-phillipsite–filled amygdules. The Fe(III) (oxy)hydroxides observed may have been produced either chemically or biologically by microbial and chemical iron(II) oxidation at a neutral pH (Emerson, 2000).

The fossilized microorganisms within vesicles of the Coral Patch pillow basalt are preserved as organic remains (carbonaceous membrane) and mineral (K-phillipsite, Ti oxides,

and Fe hydroxides)–replaced structures. Because biogenic carbonaceous matter degrades progressively and presumably continuously during mineralization and encrustation, the presence of native fluorescence from the microfossils and surrounding area indicates that the organic remains retain a sufficient number of functional groups to produce a detectable signal. Their morphologies and distribution are consistent with a biotic origin and, though it is not possible to determine exactly when they infiltrated the vesicles, their mineral composition is consistent with early microbially mediated authigenesis in a marine environment. Their microhabitat suggests that they were chemolithotrophic and heterotrophic cryptoendoliths that inhabited a low-temperature circumneutral to alkaline aqueous microhabitat.

5.5. Vesicular habitat: a suitable niche for life with high preservation potential

Life displays a wide range of survival strategies and can adapt to even the most inhospitable habitats. Endolithic environments are ubiquitous terrestrial microbial habitats and, as such, represent an important area of study in the fields of geomicrobiology, early life research, and astrobiology. Endolithic microorganisms, including cryptoendoliths, can colonize a wide variety of substratums, especially in extreme environments, and produce characteristic structures and bio-alteration textures with a high preservation potential (Friedmann and Koriem, 1989; Wynn-Williams and Edwards, 2000).

The study of terrestrial analogues of potential extraterrestrial environments is a prerequisite for astrobiology and planetary exploration. Oceanic basalt rocks are rich in reduced elements (*e.g.*, iron) that play a crucial role in the microbiology of basalt endolithic habitats. In fact, (chemolithoautotrophic) microbial alteration of oceanic basalts has a significant influence on deep-sea carbon cycling and chemical exchange between basalt and seawater (Santelli *et al.*, 2008). Oceanic volcanic rocks were prevalent on early Earth and probably on early Noachian Mars (Westall, 2005). Thus, endolithic microorganisms would be strong candidates for the colonization of early Earth and other volcanic planetary surfaces (*e.g.*, Friedmann and Koriem, 1989; Fisk *et al.*, 2006). The microhabitats within vesicles would have provided a UV-protected environment for microorganisms on planets, such as early Earth, that had no ozone shield (Cockell and Raven, 2004). Vesicles also represent environments that would have been protected from the catastrophic effects of volcanism and meteoritic impact on early Earth and Mars (Cockell *et al.*, 2002). However, the size, diversity, and functional activity of endolithic microbes on, and within, the rock substrate at the seafloor are poorly known (Edwards *et al.*, 2005). Biotic alteration morphologies, such as euendolithic microborings in Archean pillow lavas in South Africa and Western Australia (Furnes *et al.*, 2004; Banerjee *et al.*, 2006) have been described and advanced as a new astrobiological biosignature (McLoughlin *et al.*, 2007). Though euendolithic bioalteration of volcanic rock/glass surfaces has been well documented in the geological record (review in Staudigel *et al.*, 2008), fossil cryptoendoliths within vesicles of submarine basalts are little known (Schumann *et al.*, 2004; Cavalazzi *et al.*, 2008; Peckmann *et al.*, 2008; Eickmann *et al.*, 2009; this study). Cryptoendoliths have also been found to colonize vesicles of basaltic rocks in terrestrial environments (Jorge Villar *et al.*, 2006). The discovery of populated vesicles of volcanic rocks from the ocean basins and in terrestrial environments has widened the prospect of finding new sites for these extreme environments on Earth. The astrobiological relevance of fossil cryptoendoliths within vesicles in pillow is further emphasized by the finding of extremely vesicular basalt within the Columbia Hills on the Gusev Crater floor (Mars Exploration Rover Spirit mission) (Schmidt *et al.*, 2008). From this perspective, the cryptic habitat of pillow basalts and their associated microorganisms represent an, as yet, underappreciated environment in which to search for evidence of life.

6. Conclusions

Partly mineral-replaced (K-phillipsite, Fe hydroxides, and Ti oxide) filaments and spherical structures occur within K-phillipsite–filled amygdules in the chilled margin of pillow lavas from Coral Patch Seamount, eastern North Atlantic Ocean.

Well-preserved and carbonaceous filamentous and spherical structures show low variability in size and shape. Their biogenicity was assessed on recognized biogenicity criteria established for microfossils. In particular, the co-occurrence of their cellular morphologies (biomorphic features, arrangement and distribution), their mineralogical and chemical compositions, and associated autofluorescence signal and environmental microhabitat strongly support their biogenicity. The microbial population would have included lithoautotrophs and may have included mineralized sheathed microorganisms, possibly Fe-oxidizing bacteria. The presence of phillipsite and anatase permineralized microfossils, as well as anatase grains within the K-phillipsite matrix, indicates that the environment within the vesicles had a circumneutral to acidic pH.

Since the vesicles are primary structures in the altered glass of pillow basalt, the fossil microorganisms described in this study must have been cryptoendoliths, and the vesicular habitat suggests that they were chemotrophic/lithoautotrophic organisms. This type of volcanic microenvironment and the cryptoendolithic microorganisms that could inhabit it need further study. Such environments, which would have been common on early Earth and probably on early Mars, represent analogues of astrobiological interest.

Acknowledgments

We gratefully acknowledge N. Zitellini, A. Ceregato, and L. Capotondi, ISMAR-CNR Bologna for donating samples. We acknowledge funding for B.C. from CNR-CNRS International Cooperation Program, for F.W. from GDR-Exobiologie grant, and for S.L.C. from NASA under award No. NNG04GJ84G and NSF under award No. GEO0808211. Thanks are due to I. Raffi, Università di Chieti-Pescara (Italy) for help in fossil nannoplankton identification. N. McLoughlin, G. Glamoclija, and anonymous reviewers provided useful comments.

Abbreviations

CLSM, confocal laser scanning microscope; EDX, energy-dispersive X-ray; ESEM, environmental scanning electron

microscope; FEG-SEM, field emission gun scanning electron microscope; SEM, scanning electron microscope.

References

Amos, W.B. and White, J.G. (2003) How the confocal laser scanning microscope entered biological research. *Biology of the Cell* 95:335–342.

Bach, W. and Edwards, K.J. (2003) Iron and sulfide oxidation within the basaltic ocean crust: implications for chemolithoautotrophic microbial biomass production. *Geochim Cosmochim Acta* 67:3871–3887.

Banerjee, N.R. and Muehlenbachs, K. (2003) Tuff life: bioalteration in volcaniclastic rocks from the Ontong Java Plateau. *Geochemistry, Geophysics, Geosystems* 4, doi:10.1029/2002GC000470.

Banerjee, N.R., Furnes, H., Muehlenbachs, K., Staudigel, H., and de Wit, M. (2006) Preservation of ~3.4–3.5 Ga microbial biomarkers in pillow lavas and hyaloclastites from the Barberton Greenstone Belt, South Africa. *Earth Planet Sci Lett* 241:707–722.

Bedard, D.L., Bailey, J.J., Reiss, B.L., and Van Slyke Jerzak, G. (2006) Development and characterization of stable sediment-free anaerobic bacterial enrichment cultures that dechlorinate Aroclor 1260. *Appl Environ Microbiol* 72:2460–2470.

Beveridge, T.J. (1989) Role of cellular design in bacterial metal accumulation and in mineralization. *Annu Rev Microbiol* 43:147–171.

Bhartia, R., Hug, W.F., Salas, E.C., Reid, R.D., Sijapati, K.K., Tsapin, A., Abbey, W., Nealson, K.H., Lane, A.L., and Conrad, P.G. (2008) Classification of organic and biological materials with deep ultraviolet excitation. *Appl Spectrosc* 62:1070–1077.

Bhartia, R., Salas, E.C., Hug, W.F., Reid, R.D., Lane, A.L., Edwards, K.J., and Nealson, K.H. (2010) Label-free bacterial imaging with deep-UV-laser-induced native fluorescence. *Appl Environ Microbiol* 76:7231–7237.

Brasier, M., McLoughlin, N., Green, O., and Wacey, D. (2006) A fresh look at the fossil evidence for early Archaean cellular life. *Philos Trans R Soc Lond B Biol Sci* 361:887–902.

Buick, R. (1990) Microfossil recognition in Archean rocks: an appraisal of spheroids and filaments from a 3500 m.y. old chert-barite unit at North Pole, Western Australia. *Palaios* 5:441–459.

Cady, S.L., Farmer, J.D., Grotzinger, J.P., Schopf, J.W., and Steele, A. (2003) Morphological biosignatures and the search for life on Mars. *Astrobiology* 3:351–368.

Cavalazzi, B., Westall, F., and Barbieri, R. (2008) (Crypto-)Endoliths from vesicular pillow lavas, Coral Patch Seamount North Atlantic Ocean. *Studi Trent Sci Nat Acta Geol* 83:177–182.

Chan, C.S., Fakra, S.C., Emerson, D., Fleming, E.J., and Edwards, K.J. (2011) Lithotrophic iron-oxidizing bacteria produce organic stalks to control mineral growth: implications for biosignature formation. *ISME J* 5:717–727.

Cockell, C.S. and Herrera, A. (2008) Why are some microorganisms boring? *Trends Microbiol* 16:101–106.

Cockell, C.S. and Raven, J.A. (2004) Zones of photosynthetic potential on Mars and early Earth. *Icarus* 169:300–310.

Cockell, C.S., Lee, P., Osinsky, G., Horneck, H., and Broady, P. (2002) Impact-induced microbial endolithic habitats. *Meteorit Planet Sci* 37:1287–1298.

Connell, L., Barrett, A., Templeton, A., and Staudigel, H. (2009) Fungal diversity associated with an active deep sea volcano: Vailulu'u Seamount, Samoa. *Geomicrobiol J* 26:8597–8605.

Demoulin, A., Trigance, C., Neff, D., Foy, E., Dillmann, P., and L'Hostis, V. (2010) The evolution of the corrosion of iron in hydraulic binders analysed from 46- and 260-year-old buildings. *Corros Sci* 52:3168–3179.

Edwards, K.J., Bach, W., McCollom, T.M., and Rogers, D.R. (2004) Neutrophilic iron-oxidizing bacteria in the ocean: their habitats, diversity, and roles in mineral deposition, rock alteration, and biomass production in the deep-sea. *Geomicrobiol J* 21:393–404.

Edwards, K.J., Bach, W., and McCollom, T. (2005) Geomicrobiology in oceanography: microbe mineral interactions at and below the seafloor. *Trends Microbiol* 13:449–456.

Eickmann, B., Bach, W., Kiel, S., Reitner, J., and Peckmann, J. (2009) Evidence for cryptoendolithic life in Devonian pillow basalts of Variscan orogens, Germany. *Palaeogeogr Palaeoclimatol Palaeoecol* 283:120–125.

Emerson, D. (2000) Microbial oxidation of Fe(II) and Mn(II) at circumneutral pH. In *Environmental Microbe-Mineral Interactions*, edited by D.R. Lovley, ASM Press, Washington DC, pp 109–144.

Emerson, D. and Moyer, C.L. (1997) Isolation and characterization of novel iron-oxidizing bacteria that grow at circumneutral pH. *Appl Environ Microbiol* 63:4784–4792.

Emerson, D. and Moyer, C.L. (2002) Neutrophilic Fe-oxidizing bacteria are abundant at the Loihi seamount hydrothermal vents and play a major role in Fe oxide deposition. *Appl Environ Microbiol* 68:3085–3093.

Fisk, M.R., Storrie-Lombardi, M.C., Douglas, S., Popa, R., McDonald, G., and Di Meo-Savoie, C. (2003) Evidence of biological activity in Hawaiian subsurface basalts. *Geochemistry, Geophysics, Geosystems* 4, doi:10.1029/2002GC000387.

Fisk, M.R., Popa, R., Mason, O.U., Storrie-Lombardi, M.C., and Vincenzi, E.P. (2006) Iron-magnesium silicate bioweathering on Earth (and Mars?). *Astrobiology* 6:48–68.

Friedmann, E.I. and Koriem, A.M. (1989) Life on Mars: how it disappeared (if it was ever there). *Adv Space Res* 9:167–172.

Furnes, H. and Staudigel, H. (1999) Biological mediation in ocean crust alteration: how deep is the deep biosphere? *Earth Planet Sci Lett* 166:97–103.

Furnes, H., Muehlenbachs, K., Torsvik, T., Tumyr, O., and Lang, S. (2002) Bio-signatures in metabasaltic glass of a Caledonian ophiolite, West Norway. *Geol Mag* 139:601–608.

Furnes, H., Banerjee, N.R., Muehlenbachs, K., Staudigel, H., and de Wit, M. (2004) Early life recorded in Archean pillow lavas. *Science* 304:578–581.

Furnes, H., Banerjee, N.R., Staudigel, H., Muehlenbachs, K., McLoughlin, N., de Wit, M., and Van Kranendonk, M. (2007) Comparing petrographic signatures of bioalteration in recent to Mesoarchean pillow lavas: tracing subsurface life in oceanic igneous rocks. *Precambrian Res* 158:156–176.

Gaft, M., Reisfeld, R., and Panczer, G. (2005) *Modern Luminescence Spectroscopy of Minerals and Materials*, Springer, Berlin.

García Ruiz, J.M., Carnerup, A.M., Christy, A.G., Welham, N.J., and Hyde, S.T. (2002) Morphology: an ambiguous indicator of biogenicity. *Astrobiology* 2:353–369.

Geldmacher, J. and Hoernle, K. (2000) The 72 Ma geochemical evolution of the Madeira hotspot (eastern North Atlantic): recycling of Paleozoic (≤500 Ma) oceanic lithosphere. *Earth Planet Sci Lett* 183:73–92.

Glamoclija, M., Steele, A., Fries, M., Schieber, J., Voytek, M.A., and Cockell, C.S. (2009) Association of anatase (TiO_2) and microbes: unusual fossilization effect or a potential biosignature? *Geological Society of America Special Papers* 458:965–975.

Gorobets, B.S. and Rogojine, A.A., editors. (2002) *Luminescent Spectra of Minerals Reference-Book*, Coronet Books Inc., Philadelphia, PA, USA.

Ivarsson, M., Lausmaa, J., Lindblom, S., Broman, C., and Holm, N.G. (2008) Fossilized microorganisms from the Emperor

Seamounts: implications for the search for a subsurface fossil record on Earth and Mars. *Astrobiology* 8:1139–1157.
Jehlinča, J. and Bény, C. (1992) Application of Raman microspectrometry in the study of structural changes in Precambrian kerogens during regional metamorphism. *Org Geochem* 18:211–213.
Jorge Villar, S.E., Edwards, H.G.M., and Benning, L.G. (2006) Raman spectroscopic and scanning electron microscopic analysis of a novel biological colonisation of volcanic rocks. *Icarus* 184:158–169.
Kappler, A. and Straub, K.L. (2005) Geomicrobiological cycling of iron. *Reviews in Mineralogy and Geochemistry* 59:85–108.
Kashefi, K. and Lovley, D.R. (2003) Extending the upper temperature limit for life. *Science* 301:934.
Kim, J., Dong, H.L., Seabaugh, J., Newell, S.W., and Eberl, D.D. (2004) Role of microbes in the smectite-to-illite reaction. *Science* 303:830–832.
Knoll, A. (1999) Recognition of a biological signature in rocks. Discussion summary. In *Size Limits of Very Small Microorganisms: Proceedings of a Workshop,* Steering Group for the Workshop on Size Limits of Very Small Microorganisms, National Research Council, The National Academies Press, Washington DC, pp 85–87.
Konhauser, K.O. (1998) Diversity of bacterial iron mineralization. *Earth-Science Reviews* 43:91–121.
Kostka, J.E., Dalton, D.D., Skelton, H., Dollhopf, S., and Stucki, J.W. (2002) Growth of iron(III)-reducing bacteria on clay minerals as the sole electron acceptor and comparison of growth yields on a variety of oxidized iron forms. *Appl Environ Microbiol* 68:6256–6262.
Laetsch, T.A. and Downs, R.T. (2006) Software for identification and refinement of cell parameters from powder diffraction data of minerals using the RRUFF Project and American Mineralogist Crystal Structure Databases [abstract P08-25]. In *Program and Abstracts of the 19th General Meeting of the International Mineralogical Association,* International Mineralogical Association.
Marshall, C.P., Edwards, H.G.M., and Jehlinča, J. (2010) Understanding the application of Raman spectroscopy to the detection of traces of life. *Astrobiology* 10:229–243.
McLoughlin, N., Brasier, M.D., Wacey, D., Green, O.R., and Randall, S.P. (2007) On biogenicity criteria for endolithic microborings on early Earth and beyond. *Astrobiology* 7:10–26.
McLoughlin, N., Furnes, H., Banerjee, N.R., Muehlenbachs, K., and Staudigel, H. (2009) Ichnotaxonomy of microbial trace fossils in volcanic glass. *J Geol Soc London* 166:159–169.
Nielsen, M.E. and Fisk, M.R. (2010) Surface area measurements of marine basalts: implications for the subseafloor microbial biomass. *Geophys Res Lett* 37, doi:10.1029/2010GL044074.
Peck, D.L. (1978) Cooling and vesiculation of Alae Lava Lake, Hawaii. U.S. Geological Survey Professional Paper 935-B, U.S. Geological Survey, Washington DC.
Peckmann, J., Bach, W., Behrens, K., and Reitner, J. (2008) Putative cryptoendolithic life in Devonian pillow basalt, Rheinisches Schiefergebirge, Germany. *Geobiology* 6:125–135.
Santelli, C.M., Orcutt, B.N., Banning, E., Bach, W., Moyer, C.L., Sogin, M.L., Staudigel, H., and Edwards, K.J. (2008) Abundance and diversity of microbial life in ocean crust. *Nature* 453:653–656.
Schmidt, M.E., Ruff, S.W., McCoy, T.J., Farrand, W.H., Johnson, J.R., Gellert, R., Ming, D.W., Morris, R.V., Cabrol, N., Lewis, K.W., and Schroeder, C. (2008) Hydrothermal origin of halogens at Home Plate, Gusev Crater. *J Geophys Res* 113, doi:10.1029/2007JE003027.
Schopf, J.W., Kudryavtsev, A.B., Agresti, D.G., Czaja, A.D., and Wdowiak, T.J. (2005) Raman imagery: a new approach to assess the geochemical maturity and biogenicity of permineralized Precambrian fossils. *Astrobiology* 5:333–371.
Schopf, J.W., Tripathi, A.B., and Kudryavtsev, A.B. (2006) Three-dimensional confocal optical imagery of Precambrian microscopic organisms. *Astrobiology* 6:1–16.
Schopf, J.W., Kudryavtsev, A.B., Czaja, A.D., and Tripathi, A.B. (2007) Evidence of Archean life: stromatolites and microfossils. *Precambrian Res* 158:141–155.
Schopf, J.W., Kudryavtsev, A.B., and Sergeev, V.N. (2010a) Confocal laser scanning microscopy and Raman imagery of the late Neoproterozoic Chichkan microbiota of South Kazakhstan. *J Paleontol* 84:402–416.
Schopf, J.W., Kudryavtsev, A.B., Sugitani, K., and Walter, M.R. (2010b) Precambrian microbe-like pseudofossils: a promising solution to the problem. *Precambrian Res* 179:191–205.
Schumann, G., Manz, W., Reitner, J., and Lustrino, M. (2004) Ancient fungal life in North Pacific Eocene oceanic crust. *Geomicrobiol J* 21:241–246.
Shabtai, Y. and Fleminger, G. (1994) Adsorption of *Rhodococcus* strain GIN-1 (NCIMB 40340) on titanium dioxide and coal fly ash particles. *Appl Environ Microbiol* 60:3079–3088.
Staudigel, H., Furnes, H., McLoughlin, N., and Banerjee, N.R. (2008) 3.5 billion years of glass bioalteration: volcanic rocks as basis for microbial life? *Earth-Science Reviews* 89:156–176.
Stroncik, N.A. and Schmincke, H.-U. (2001) Evolution of palagonite: crystallization, chemical changes, and elemental budget. *Geochemistry, Geophysics, Geosystems* 2, doi:10.1029/2000GC000102.
Summons, R.E, Jahnke, L.L, Hope, M., and Logan, G.A. (1999) 2-Methylhopanoids as biomarkers for cyanobacterial oxygenic photosynthesis. *Nature* 400:554–557.
Takai, K., Moser, D.P., DeFlaun, M.F., Onstott, T.C., and Fredrickson, J.K. (2001) Archaeal diversity in waters from deep South African gold mines. *Appl Environ Microbiol* 67: 5750–5760.
Thorseth, I.H., Torsvik, T., Furnes, H., and Muehlenbachs, K. (1995) Microbes play an important role in the alteration of oceanic crust. *Chem Geol* 126:137–146.
Thorseth, I.H., Torsvik, T., Torsvik, V., Daae, F.L., and Pedersen, R.B. (2001) Keldysh-98 scientific party, diversity of life in ocean floor basalt. *Earth Planet Sci Lett* 194:31–37.
van Veen, W.L., Mulder, *E.G.,* and Deinema, M.H (1978) The *Sphaerotilus-Leptothrix* group of bacteria. *Microbiol Rev* 42: 329–356.
Westall, F. (2005) Early life on Earth and analogies to Mars. In *Water on Mars and Life,* Advances in Astrobiology and Biogeophysics 4, edited by T. Tokano, Springer, Berlin, pp 45–64.
Wynn-Williams, D.D. and Edwards, H.G.M. (2000) Antarctic ecosystems as models for extraterrestrial surface habitats. *Planet Space Sci* 48:1065–1075.

Address correspondence to:
Barbara Cavalazzi
Department of Geology
University of Johannesburg
Johannesburg
South Africa

E-mail: cavalazzib@uj.ac.za

Submitted 26 March 2011
Accepted 2 July 2011